

Astragaloside IV Attenuates Angiotensin II-Induced Inflammatory Responses in Endothelial Cells: Involvement of Mitochondria

Shiyu Zhang , Shijie Li , Lin Cui , Shiyang Xie , Youping Wang 

Division of Cardiology and Central Laboratory, First Affiliated Hospital, Henan University of Traditional Chinese Medicine, Zhengzhou, 450000, People's Republic of China

Correspondence: Youping Wang, Division of Cardiology and Central Laboratory, First Affiliated Hospital, Henan University of Traditional Chinese Medicine, 19 Renmin Road, Zhengzhou, 450000, People's Republic of China, Tel +86-371-66248345, Email wangyp8@163.com

Background: Angiotensin II (Ang II)-triggered endothelial inflammation is a critical mechanism contributing to Ang II-related cardiovascular diseases. The inflammation is highly correlated with mitochondrial function. Although astragaloside IV (AS-IV), a primary bioactive ingredient extracted from the traditional Chinese medicine *Astragalus membranaceus* Bunge that can effectively treat numerous cardiovascular diseases, possesses the actions of antiinflammation and antioxidation in vivo, limited data are made available on the impacts of AS-IV on mitochondrial function in endothelial inflammation triggered by Ang II. This study was performed to evaluate the in vitro actions of AS-IV on Ang II-triggered inflammatory responses in endothelial cells, and to further clarify the potential role of mitochondria in the actions.

Methods: Human umbilical vein endothelial cells (HUVECs) were preincubated with AS-IV and then exposed to Ang II for 12 h.

Results: The exposure of HUVECs to Ang II triggered cytokine and chemokine production, the upregulation of adhesive molecules, monocyte attachment, and nuclear factor-kappa B activation. Additionally, our results showed that the inflammatory responses triggered by Ang II were associated with the impairment of mitochondrial function, as evidenced by the reductions of mitochondrial membrane potential, ATP synthesis, and mitochondrial complexes I and III activities. Moreover, the concentrations of malondialdehyde, cellular reactive oxygen species, and mitochondrial superoxide enhanced after HUVECs challenged with Ang II, which were concurrent with the decreases in total superoxide dismutase (SOD) and its isoenzyme activities such as Mn-SOD. These Ang II-induced alterations were reversed by preincubation with AS-IV.

Conclusion: Our data indicate that AS-IV attenuates Ang II-triggered endothelial inflammation possibly via ameliorating mitochondrial function.

Keywords: astragaloside IV, angiotensin II, mitochondria, inflammation, endothelial cells

Introduction

In the world, cardiovascular diseases remain the major causes of morbidity and mortality.^{1,2} Inflammation, as a significant hallmark of endothelial injury, is recognized to contribute to the development of cardiovascular diseases.^{3,4} Numerous studies demonstrate that the disruption of endothelial cell homeostasis, a condition defined as endothelial dysfunction, contributes to the pathogenesis of various inflammation-characterized circulatory disorders, including atherosclerosis, hypertension, and ischemia-reperfusion injury.⁴⁻⁶ Currently, endothelial dysfunction is thought to be the critical initiating factor for inflammation and frequently associated with mitochondrial dysfunction.^{7,8} Mitochondrial reactive oxygen species (ROS) are involved in the development of multiple diseases characterized by inflammation, and mitochondrial ROS scavengers have been demonstrated to inhibit inflammatory responses.^{5,8-10} These results indicate that mitochondrial dysfunction can cause various pathological processes, including inflammation, through increased mitochondrial ROS production. Under pathological conditions, mitochondrial ROS are primarily derived from abnormal oxidative phosphorylation occurring in mitochondria. Mitochondrial dysfunction, as a main source of ROS, is

frequently derived from the changes in mitochondrial energy metabolism, ATP synthesis, mitochondrial membrane potential (MMP), and mitochondrial biogenesis.¹⁰

It is well established that angiotensin II (Ang II), the principal component of the renin-angiotensin-aldosterone system, is implicated in a series of physiological and pathophysiological processes, including sodium and water homeostasis, inflammation, and a number of cardiovascular diseases.¹¹ It is well accepted that Ang II is one of the critical pathological stimulus for inflammation.^{11,12} Results from in vivo and in vitro studies show that mitochondrial ROS is involved in Ang II-induced injury in various tissues.^{5,13,14} Thus, important for the pathogenic effects of Ang II, is its ability to enhance ROS generation by triggering mitochondrial dysfunction in various tissues, including endothelium. Although the detailed mechanisms responsible for Ang II-mediated inflammatory response are unelucidated, mitochondrial dysfunction appears to be one of the attractive mechanisms for Ang II-triggered inflammation, which is accompanied by an enhancement of ROS formation.¹⁵

Astragaloside IV (AS-IV) is a primary ingredient extracted from *Astragalus membranaceus* Bunge, which has been commonly utilized in the clinic for the therapy for numerous cardiovascular diseases in China.¹⁶ In addition to its antioxidant and myocardial protective properties,^{16–18} AS-IV has been shown to ameliorate Ang II- and diabetes-induced organ injury, including aortic aneurysm and renal damage.^{19–21} The protective actions of AS-IV are attributed to its antiinflammatory properties. It is well accepted that the pathogenesis of inflammation is mediated by many factors, including mitochondrial dysfunction and its ROS production. Recently, it has been recognized that Ang II can cause damage to mitochondria, thereby leading to the overproduction of mitochondrial ROS under pathological conditions. Although it is possible that AS-IV acts as an antioxidant agent to ameliorate mitochondrial dysfunction,^{22,23} limited data are available for Ang II-induced inflammation regarding the relationship between AS-IV and mitochondrial function.

Given the critical role of endothelial function in the pathogenesis of inflammation, an in vitro model of human umbilical vein endothelial cells (HUVECs) was employed to determine the in vitro actions of AS-IV on endothelial inflammation triggered by Ang II, and to further clarify the mitochondria potentially implicated in the actions in this study.

Materials and Methods

Chemical and Reagents

AS-IV, its purity determined by NMR $\geq 98\%$, was supplied by MedChemExpress (Monmouth Junction, NJ, USA). Dimethyl sulfoxide (DMSO), 3-(4,5-dimethylthiazol-2-yl)-2,5-diphenyltetrazolium bromide (MTT), and mitochondria isolation kit were provided by Sigma Chemical (St. Louis, MO, USA). A EGM-2 Bullet kit was from Lonza (Allendale, NJ, USA). RPMI-1640 medium, carboxyfluorescein diacetate succinimidyl ester (CDSE), fetal bovine serum (FBS), lipophilic cationic dye JC-1, DCFH-DA probe, and MitoSOX Red were all supplied by Invitrogen (Carlsbad, CA, USA). A protein assay kit and RIPA lysis buffer were supplied by Bio-Rad Laboratories (Hercules, CA, USA) and Thermo Scientific (Waltham, MA, USA), respectively. Cytokine and chemokine ELISA kits were provided by R&D Systems (Minneapolis, MN, USA). The mouse monoclonal antibodies against ICAM-1 and VCAM-1 were purchased from Santa Cruz Biotechnology (Santa Cruz, CA, USA). The FITC-conjugated antimouse antibody was obtained from Jackson ImmunoResearch Laboratories (West Grove, PA, USA). The specific TransAM NF- κ B p65 transcription factor assay kit and nuclear extraction kit were supplied by Active Motif (Carlsbad, CA, USA). The mitochondrial complex I enzyme activity microplate assay kit and complex III activity assay kit were supplied by Abcam (Cambridge, MA, USA). The luminescence-based ATP assay kit, CuZn/Mn-SOD kit (WST-8), and lipid peroxidation MDA assay kit were provided by Beyotime Biotechnology (Shanghai, China).

Cell Lines and Study Protocols

HUVECs from Lonza (Allendale, NJ, USA) were allowed to grow in a growth supplement-containing EGM-2 Bullet kit medium. HUVECs between 3 to 7th passages were utilized in the whole study. For starvation, HUVECs, at 80–90% confluence, were cultured in the EGM-2 Bullet kit medium without growth supplements for 4 h prior to the start of the experiments. According to the manufacturer's suggestions, THP-1 (a human monocytic cell line; $2\text{--}5 \times 10^6$ cells/mL;

ATCC, Manassas, VA, USA) was grown in 10% FBS-containing RPMI-1640 medium. To maintain sufficient cell growth, the cells mentioned above were routinely grown at 37°C in a humidified incubator with 5% carbon dioxide.

AS-IV was dissolved in the solvent DMSO (1 mg/mL) and kept at -20°C. To reach the desired concentrations, the stock solutions were serially diluted using the culture medium for the experiments. HUVECs at 80–90% confluence were incubated with AS-IV (3, 10, or 30 µM) for 1 h prior to Ang II (1 µM) exposure for the indicated times. Incubation of HUVECs with DMSO alone was used as controls.

Determination of Cell Viability

An MTT colorimetric assay was used to determine cell viability as originally described by Mosmann.²⁴ Briefly, HUVECs at a density of 1×10^4 cells/well were cultured in 96-well plates for 12 h. Following exposure of HUVECs to AS-IV at various concentrations for the indicated times, the MTT reagent at the final concentration of 0.5 mg/mL was distributed into each well and cocultured for an additional 4 h. Next, the MTT reagent-containing medium was aspirated, DMSO (100 µL) was added to bring the formazan crystals into the solution. After that, a SpectraMax microplate reader (Molecular Devices, Sunnyvale, CA, USA) was used to determine the amount of formazan at 570 nm. Cell viability was expressed as a percentage with the unstimulated cells as 100%.

Determination of Cytokine and Chemokine Levels

To measure the levels of cytokines and chemokines, the cell culture condition media were collected 12 h after exposure of HUVECs (3×10^5 cells/well) to Ang II with or without AS-IV in 6-well plates. The commercial ELISA kits were applied to determine the levels of cytokines (TNF-α and IL-6), and chemokines (MCP-1). The levels of cytokines and chemokines were reported as pg/mL of the media.

Determination of Adhesion Molecule Expression

The influence of AS-IV on the Ang II-triggered expression of adhesion molecules was evaluated by the use of a cell-based ELISA assay per our previous publication.^{25,26} Briefly, 4% paraformaldehyde was used to fix HUVECs in a 96-well plate for 5 min after 12 h of incubation of the cells with Ang II. To permeabilize the fixed HUVECs, the cells were incubated with the prechilled methanol for 10 min at 4°C. After then, the cells were blocked using phosphate-buffered saline (PBS) with 1% BSA and 0.2% Triton X-100 for 1 h before incubation of them with mouse monoclonal antibody directed to ICAM-1 or VCAM-1 (dilutions, 1:100) for 12 h at 4°C. After rinsing with PBS, FITC-conjugated secondary antibody directed to mouse (dilution, 1:200) was incubated for 1 h at room temperature. The optical density of each well was determined at excitation 485 nm/emission 520 nm with a SpectraMax microplate reader. Results were reported as fold alterations relative to the unstimulated group.

Evaluation of Monocyte Adhesion

The measurement of monocyte attachment was carried out as previously described.^{25,26} Briefly, HUVECs (1×10^4 cells/well) were routinely grown in 96-well plates overnight before 12 h of exposure of the cells to Ang II with or without AS-IV (3, 10, or 30 µM). CDSE (1 µM) was used to fluorescently label THP-1 at 37°C for 30 min before applying the THP-1 to the HUVECs challenged with Ang II. Next, the THP-1 cells labeled with CDSE were cocultured with HUVECs exposed to Ang II at 37°C for 30 min under normal culture conditions. To lyse the THP-1 cells, the cells were incubated with 2% Triton X-100-containing PBS after rinsing with PBS. A SpectraMax microplate reader was used to determine the total fluorescence levels of the cell lysates at 485/520 nm. Data were recorded as fold alterations of the intensity of fluorescence relative to the unstimulated group. In addition, HUVECs at a density of 0.5×10^5 cells/well were allowed to grow in 24-well plates. The experiments were performed to determine the adhesion of fluorescence-labeled THP-1 cells to endothelial cells as described above. Eventually, after removing the non-attached pre-stained THP-1 cells, a fluorescent inverted microscope was used to visualize the attached THP-1 cells at 485/535 nm.

Determination of the Activity of Nuclear Factor-Kappa B (NF- κ B) p65 Binding to DNA

HUVECs (3×10^5 cells/well) grown in 6-well plates were incubated with AS-IV (3, 10, or 30 μ M) before 30 min of Ang II exposure. After then, according to the manufacturer's instructions, the nuclear extraction kit obtained from Active Motif (Carlsbad, CA, USA) was applied to extract nuclear protein from the cells. A protein assay kit was used to determine the levels of nuclear protein. The activity of NF- κ B p65 binding to DNA was determined using the specific TransAM NF- κ B p65 transcription factor assay kit following the manufacturer's suggestions. The protein concentration of nuclear protein was applied to normalize the activity of NF- κ B p65 binding to DNA.

Evaluation of Mitochondrial Membrane Potential (MMP)

The lipophilic cationic dye JC-1 was used to determine the endothelial MMP as described previously.²⁷ JC-1, normally green fluorescent dye, forms red fluorescent aggregates in response to higher MMP. Therefore, the ratio between the red (J-aggregate) and green (J-monomer) fluorescence of cells loaded with JC-1 is often used for the determination of the MMP. Briefly, HUVECs (3×10^5 cells/well) cultured in 6-well plates were exposed to Ang II (1 μ M) with or without AS-IV (3, 10, or 30 μ M) for 12 h. After being washed with PBS, the cells were incubated with the JC-1 probe (2 μ M final concentration)-containing medium at 37°C for 20 min. After rinsing with PBS, a fluorescence microscope was used to visualize the JC-1-stained cells for J-aggregate at excitation 585 nm/emission 590 nm and J-monomer at excitation 515 nm/emission 529 nm, respectively. The software of ImageJ (NIH, Bethesda, MD, USA) was applied to determine the fluorescence intensity. The ratio of J-aggregate to J-monomer was used to calculate the relative MMP of endothelial cells. Results were presented as fold changes in the MMP relative to the unstimulated group.

Determination of Intracellular ATP Level

Following the product specification sheet supplied by the vendor, a luminescence-based ATP assay kit was used to determine the concentration of intracellular ATP. Briefly, HUVECs at a density of 3×10^5 cells/well grown in 6-well plates were incubation with Ang II (1 μ M) as mentioned above. Subsequently, the HUVECs were incubated in ATP assay lysis buffer provided by the kit to lyse the cells and then centrifuged at $12000 \times g$ for 10 min to get the supernatants. A protein assay kit was used to determine the protein level of the supernatant. ATP detection working solution (100 μ L) supplied by the kit was incubation with the supernatants (20 μ L) in 96-well plates. After incubation at room temperature in the dark, a TD-20/20 luminometer (Turner BioSystems, Sunnyvale, CA, USA) was used to make measurements. Following the manufacturer's instructions, a standard curve of ATP was used to calculate the levels of ATP. The ATP levels were reported as nM/mg protein.

Determination of Cellular Malondialdehyde (MDA) Level and Superoxide Dismutase (SOD) Activity

HUVECs at a density of 3×10^5 cells/well in 6-well plates were washed with PBS and harvested 12 h after exposure to Ang II with or without AS-IV (3, 10, or 30 μ M). To prepare cell lysates, a proteinase inhibitor-containing RIPA was used to resuspend the cells. The lysis was subjected to five cycles of thawing in a 37°C water bath followed by fast freezing in liquid nitrogen. A protein assay kit was used to measure the protein levels of the lysates to normalize the concentrations of MDA and activities of total SOD and its isoenzymes. Then, the lysates were stored at -80°C until measurement.

A lipid peroxidation MDA assay kit was applied to quantify the concentrations of MDA. In this method, the lysates (100 μ L) were incubated with 200 μ L aliquot of the assay solution at 100°C for 15 min. After cooling to room temperature, the mixtures were centrifuged at $1000 \times g$ for 10 min to collect the supernatants. After a 200 μ L aliquot of the supernatant was transferred to a 96-well plate, the absorbance was immediately measured at 532 nm using a SpectraMax microplate reader. The levels of MDA was calculated using a standard curve of MDA following the manufacturer's instructions.

The activities of total SOD, CuZn-SOD, and Mn-SOD were assayed using a CuZn/Mn-SOD kit (WST-8). Briefly, a 20 μ L aliquot of the lysate was mixed with 180 μ L reaction mixture supplied by the kit. This allows for a reaction with

SOD in the lysate. A SpectraMax microplate reader was used to assay the absorbance of the mixture at 450 nm after incubation at 37°C for 30 min. To determine the activity of Mn-SOD, the activity of CuZn-SOD was completely attenuated by the addition of an inhibitory solution supplied by the kit. The measurement of Mn-SOD activity was conducted as described above. The activity of Mn-SOD was subtracted from the total SOD activity to determine the activity of CuZn-SOD. SOD activity was recorded as units per milligram of protein.

Determination of Cellular ROS Level

Cellular ROS were detected using DCFH-DA probe. The intracellular levels of ROS were determined using the DCFH-DA probe 12 h after exposure of HUVECs in 6-well plates to Ang II with or without AS-IV (3, 10, or 30 μ M). After being rinsed with PBS, the cells were incubated in PBS with the DCFH-DA probe (5 μ M) at 37°C for 30 min in the dark. After rinsing with PBS, a fluorescence microscope was used to immediately visualize the DCFH-DA-stained cells at excitation/emission wavelengths of 492/520 nm. The software of ImageJ (NIH, Bethesda, MD, USA) was applied to analyze the intensity of DCFH-DA fluorescence. Results were reported as fold alterations of the fluorescence intensity relative to the unstimulated cells.

Determination of Mitochondrial Superoxide Level

Following manufacturer's suggestions, MitoSOX Red, a mitochondrial superoxide indicator, was used to determine the levels of mitochondrial superoxide. Briefly, HUVECs in 6-well plates were rinsed with 1 \times HBSS containing calcium and magnesium 12 h after incubation of the cells with Ang II with or without AS-IV (3, 10, or 30 μ M). Subsequently, the cells were fluorescently labeled with MitoSOX Red (1 μ M final concentration) diluted in 1 \times HBSS at 37°C for 10 min. After rinsing with 1 \times HBSS, a fluorescence microscope was used to observe the cells labeled with MitoSOX Red at excitation/emission wavelengths of 510/580 nm. The software of ImageJ (NIH, Bethesda, MD, USA) was applied to evaluate the fluorescent intensity, and then it was normalized to the control to produce a fold-change value.

Determination of Mitochondrial Complexes I and III Activities

To determine the activities of mitochondrial complexes I and III, HUVECs (3×10^5 cells/well) grown in 6-well plates were incubated with Ang II as described above. The mitochondria of HUVECs were extracted using the mitochondria isolation kit 12 h after exposure of HUVECs to Ang II. The mitochondria were collected in the sediments following the manufacturer's suggestions. According to the manufacturer's protocol, the complex I enzyme activity microplate assay kit and mitochondrial complex III activity assay kit were used to measure the activities of mitochondrial complexes I and III, respectively. The activity of complex I was reported as the alterations of absorbance per minute per amount of sample loaded into the well. According to the manufacturer's instructions, a standard curve of reduced cytochrome c was used to calculate the activity of complex III. Data were presented as units per milligram of protein.

Statistical Analysis

All results from at least 3 independent experiments are expressed as means \pm SE. Statistical analysis of the significance between more than 2 groups was made by one-way ANOVA followed by Bonferroni's adjustment for multiple comparisons. For all measurements, differences were considered statistically significant at $p < 0.05$. The data were analyzed by the use of GraphPad Prism software (Version 6.0; GraphPad Software, Inc., La Jolla, CA, USA).

Results

AS-IV Reduces the Viability of HUVECs

The viability of HUVECs, determined by MTT assay, was decreased 24 h following incubation with 30 μ M AS-IV (Figure 1). However, the viability of HUVECs was not found to change 6 or 12 h after incubation of HUVECs with AS-IV (3, 10, 30 μ M). In addition, to establish an in vitro model of endothelial inflammation, HUVECs were usually stimulated by Ang II (1 μ M), an inflammatory agent able to trigger inflammation. Based on these findings, in this study we chose Ang II (1 μ M), AS-IV (3–30 μ M), and an incubation period of 12 h to more fully clarify the events.

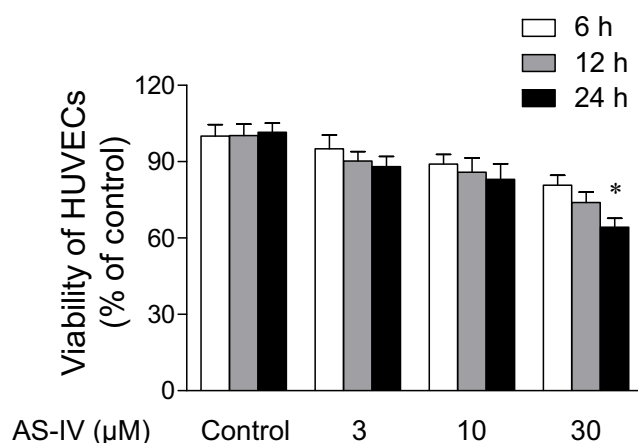


Figure 1 Effect of astragaloside IV (AS-IV) on the viability of human umbilical vein endothelial cells (HUVECs). HUVECs were incubated with AS-IV (3, 10, or 30 μM) for the indicated times. Cell viability was determined by a 3-(4,5-dimethylthiazol-2-yl)-2,5-diphenyltetrazolium bromide assay. Results are expressed as means ± SE. * $p < 0.05$ compared with the corresponding control group.

AS-IV Suppresses Ang II-Triggered Inflammation in HUVECs

The attenuating effect of AS-IV on endothelial inflammation triggered by Ang II was determined in the current study. AS-IV (3–30 μM) was found to concentration-dependently inhibit the production/expression of proinflammatory mediators, including cytokines (TNF- α and IL-6), chemokines (MCP-1), and adhesion molecules (ICAM-1 and VCAM-1), in HUVECs exposed to Ang II (Figures 2 and 3). Based on the fact that inflammatory cell adhesion to endothelial cells is a pivotal step in the development of inflammation, we evaluated the effect of AS-IV on the Ang II-mediated monocyte adhesion to HUVECs in the current study. As demonstrated in Figure 4, incubation with Ang II enhanced the number of monocytes that adhered to HUVECs. However, the AS-IV preincubation concentration-dependently suppressed monocyte adhesion triggered by Ang II. Moreover, the nuclear transcription factor NF- κ B is thought to be implicated in the generation of inflammatory factors. The NF- κ B p65 binding to DNA is necessary for the NF- κ B activation. Since the activation of NF- κ B plays an important role in the process of inflammation, the action of AS-IV in the inhibition of Ang II-triggered NF- κ B activation was evaluated by determining the DNA-binding activity of NF- κ B p65. As shown in Figure 4C, the activity of NF- κ B p65 binding to DNA increased 30 min after exposure of HUVECs to Ang II, and this action was, in a concentration-dependent manner, attenuated by AS-IV preincubation. Collectively, these data demonstrate that AS-IV can inhibit the inflammation triggered by Ang II in endothelial cells.

AS-IV Ameliorates the Mitochondrial Dysfunction Triggered by Ang II in HUVECs

Since MMP is closely related to mitochondrial function, especially mitochondrial ATP synthesis, the impacts of AS-IV on Ang II-triggered changes in MMP and mitochondrial ATP synthesis were determined in this study. As demonstrated in Figure 5, compared with the control group, Ang II stimulation for 12 h triggered an obvious decrease in the MMP of endothelial cells. Consistent with MMP alterations, ATP synthesis diminished after Ang II stimulation when compared with control unstimulated cells, while the Ang II-mediated decreases in MMP and ATP production were reversed by preincubation with AS-IV. However, incubation with AS-IV alone had no impact on MMP and ATP synthesis in HUVECs under basal unstimulated conditions. These findings highlight preincubation with AS-IV was able to ameliorate the Ang II-triggered mitochondrial dysfunction by counteracting the decreases in MMP and ATP synthesis.

AS-IV Suppresses Ang II-Triggered Increases in the Levels of Mitochondrial Oxidative Stress in HUVECs

To determine the protective actions of AS-IV on endothelial oxidative stress under inflammatory conditions triggered by Ang II, the impacts of AS-IV on oxidative damage, cytosolic ROS, mitochondrial superoxide, and SOD activities were evaluated 12 h after exposure of HUVECs to Ang II. The overproduction of cellular ROS frequently led to the peroxidation of cellular

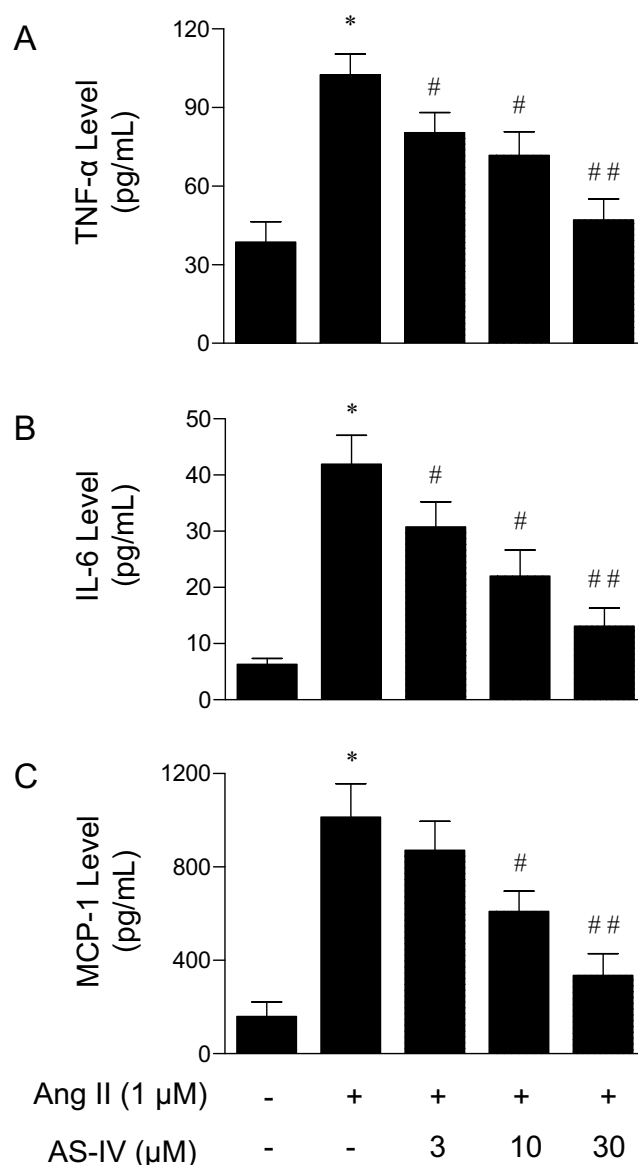


Figure 2 Effect of astragaloside IV (AS-IV) on angiotensin II (Ang II)-induced production of proinflammatory cytokines/chemokines including TNF- α (**A**), IL-6 (**B**), and MCP-1 (**C**) in endothelial cells. Human umbilical vein endothelial cells (HUVECs) were preincubated with or without AS-IV (3, 10, or 30 μ M) 1 h before incubation with Ang II (1 μ M) for 12 h. The ELISA assay was used to measure the levels of proinflammatory cytokines/chemokines in the culture medium. Results are expressed as means \pm SE. * p < 0.05 compared with the control group; # p < 0.05 and ## p < 0.01 compared with HUVECs exposed to Ang II alone.

lipids, which was determined by assaying the concentration of MDA produced from lipid peroxidation. Ang II stimulation for 12 h significantly enhanced the production of MDA, intracellular ROS, and mitochondrial superoxide when compared with control unstimulated cells (Figures 6 and 7). However, preincubation with AS-IV concentration-dependently inhibited the Ang II-mediated production of MDA, cytosolic ROS, and mitochondrial superoxide. Conversely, incubation with Ang II lowered the endothelial activity of SOD, including total SOD, Mn-SOD, and CuZn-SOD (Figure 8). All Ang II-mediated actions were reversed by AS-IV preincubation with the exception of those on CuZn-SOD activity. Collectively, the results show that AS-IV preincubation can suppress Ang II-triggered inflammation possibly via attenuating mitochondrial ROS production and increasing antioxidative enzyme activity.

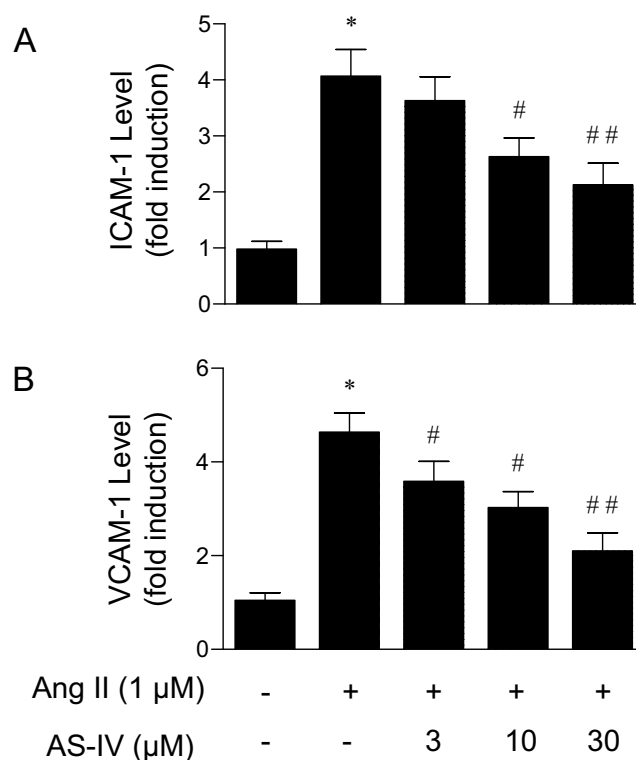


Figure 3 Effect of astragaloside IV (AS-IV) on angiotensin II (Ang II)-induced ICAM-1 (**A**) and VCAM-1 (**B**) expression in endothelial cells. Human umbilical vein endothelial cells (HUVECs) were preincubated with or without AS-IV (3, 10, or 30 μM) 1 h before incubation with Ang II (1 μM) for 12 h. The cell-based ELISA assay was used to determine the expression of ICAM-1 and VCAM-1 in HUVECs. Results are expressed as means ± SE. * $p < 0.05$ compared with the control group; # $p < 0.05$ and ## $p < 0.01$ compared with HUVECs exposed to Ang II alone.

AS-IV Attenuates Ang II-Triggered Decreases in Complexes I and III Activities in HUVECs

Because it is well established that mitochondrial superoxide is derived from respiratory chain, especially complexes I and III, the complexes I and III activities were measured 12 h after exposure of HUVECs to Ang II. As compared with unstimulated cells, HUVECs after 12 h of Ang II exposure exhibited the decreases in complexes I and III activities (Figure 9). However, preincubation with AS-IV concentration-dependently inhibited the Ang II-triggered reductions of complexes I and III activities. Collectively, these data indicate that AS-IV suppresses Ang II-mediated formation of mitochondrial ROS possibly via ameliorating the activities of complexes I and III.

Discussion

Inflammation is still a complicated issue in the development of numerous diseases. Multiple mechanisms are proposed to mediate the complexity of cellular events that result in the pathogenesis of inflammation. Among these mechanisms, mitochondrial dysfunction is considered to be one of the most critical mechanisms contributing to the progression of inflammatory responses. In the current study, our data demonstrated that AS-IV attenuates the inflammatory responses induced by Ang II as a result of its inhibiting the production of inflammatory mediators and leukocyte attachment to endothelial cells after Ang II exposure. Most importantly, these alterations were concurrent with the AS-IV-mediated improvement of mitochondrial function, characterized by increased MMP and ATP synthesis, and decreased mitochondrial ROS production. Collectively, these novel findings indicate that AS-IV suppresses endothelial inflammation triggered by Ang II possibly via the amelioration of mitochondrial function.

Inflammation is thought to contribute to the pathogenesis of circulatory disorders, including atherosclerosis, hypertension, and ischemia-reperfusion injury. Ang II is a critical pathological stimulus for cardiovascular diseases and involved in the development of various circulatory disorders involving its proinflammatory action.²⁸ Usually, Ang II

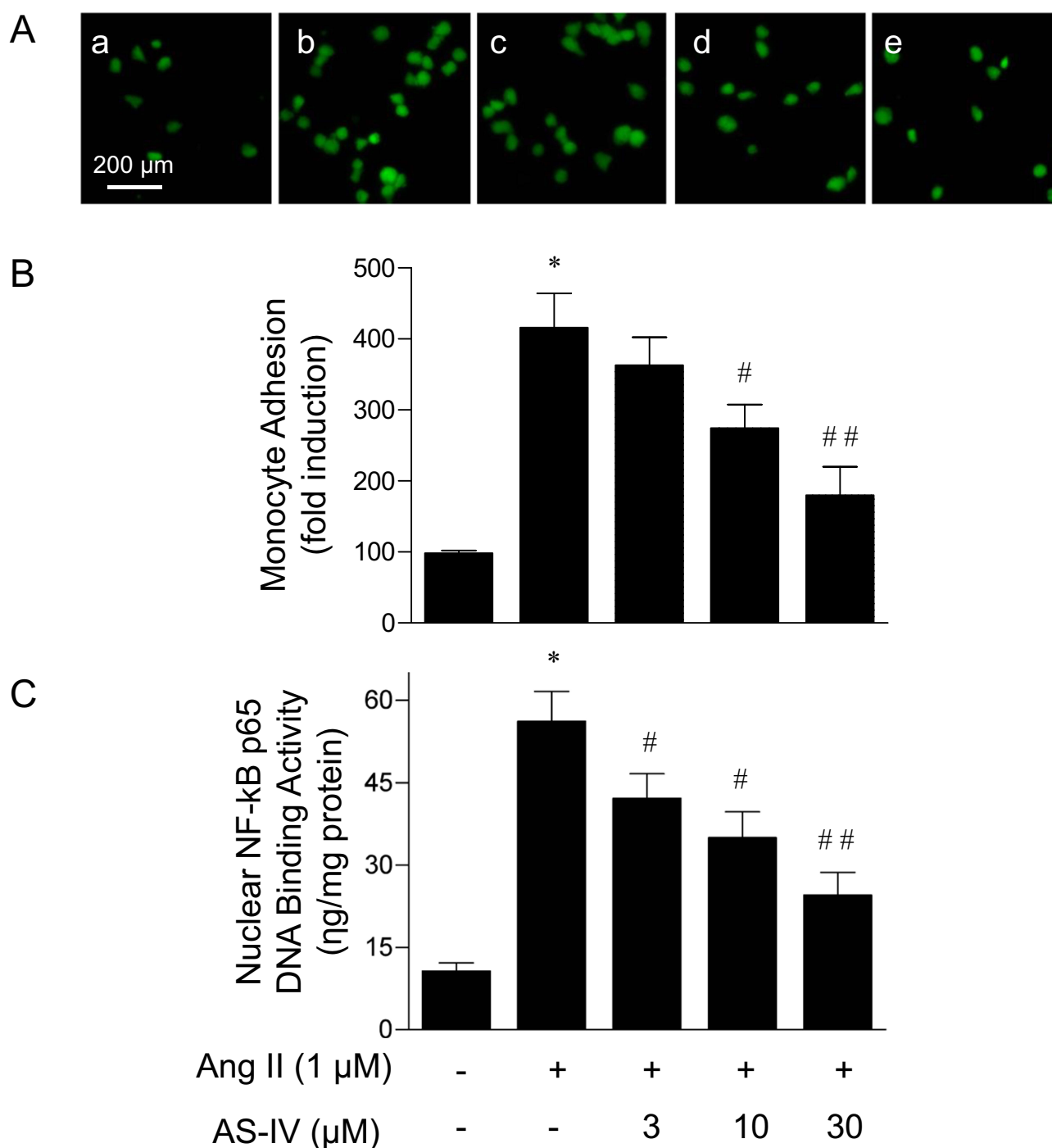


Figure 4 Effect of astragaloside IV (AS-IV) on angiotensin II (Ang II)-induced monocyte adhesion to endothelial cells (**A** and **B**) and the activation of NF-κB (**C**) in endothelial cells. Human umbilical vein endothelial cells (HUVECs) were preincubated with or without AS-IV (3, 10, or 30 μM) 1 h before incubation with Ang II (1 μM) for 12 h or 30 min. Subsequently, HUVECs were coincubated with fluorescence-labeled human monocytes for 30 min or the NF-κB activity in HUVECs was assayed by the use of a nonradioactive ELISA-based assay kit. (**A**) Fluorescent images of monocyte adhesion to HUVECs were visualized with a fluorescence microscope at 485/535 nm. Magnification, × 200. HUVECs were incubated with (a) a vehicle (control), (b) Ang II alone, Ang II with AS-IV at the concentration of (c) 3, (d) 10, or (e) 30 μM before coincubation with fluorescence-labeled monocytes. (**B**) Fluorescence intensity of monocyte attachment to HUVECs was quantified using a spectrofluorometer. (**C**) The activities of NF-κB in HUVECs were assayed using a specific TransAM NF-κB p65 transcription factor assay kit. Results are expressed as means ± SE. **p* < 0.05 compared with the control group; #*p* < 0.05 and ##*p* < 0.01 compared with HUVECs exposed to Ang II alone.

triggers the mitochondrial dysfunction of endothelial cells via binding to type-1 angiotensin receptors (AT1R) on endothelial cells. The mitochondrial superoxide anion ($O_2^{\cdot-}$) derived from mitochondrial dysfunction activates NF-κB, thereby inducing endothelial inflammation.^{13,29} In addition to the generation of inflammatory factors, a vital response

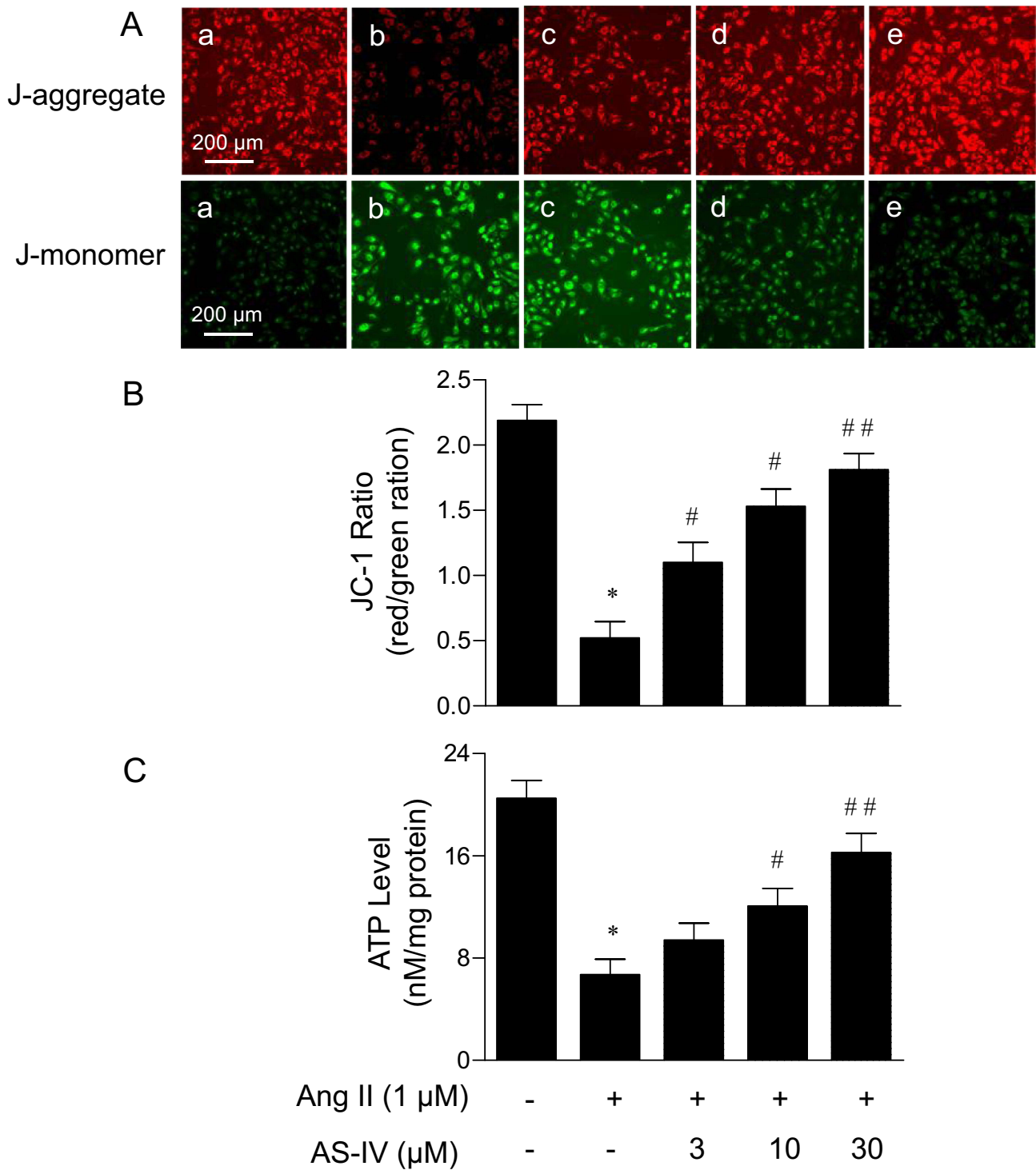


Figure 5 Effect of astragaloside IV (AS-IV) on angiotensin II (Ang II)-induced changes in mitochondrial membrane potential (MMP) (**A** and **B**) and ATP levels (**C**) in endothelial cells. Human umbilical vein endothelial cells (HUVECs) were preincubated with or without AS-IV (3, 10, or 30 μ M) 1 h before incubation with Ang II (1 μ M) for 12 h. Subsequently, HUVECs were subjected to JC-1 staining or the measurement of ATP levels in HUVECs using a commercial assay kit as described in Materials and Methods. (**A**) Fluorescent images of HUVECs stained with JC-1 were visualized with a fluorescence microscope. Magnification, \times 200. HUVECs were incubated with (a) a vehicle (control), (b) Ang II alone, Ang II with AS-IV at the concentration of (c) 3, (d) 10, or (e) 30 μ M before being stained with JC-1. (**B**) Fluorescence intensities of green and red signals were quantified for each image using ImageJ software. The relative MMP was calculated as the ratio of red (J-aggregate) to green (J-monomer). Results are expressed as means \pm SE. * p < 0.05 compared with the control group; # p < 0.05 and ## p < 0.01 compared with HUVECs exposed to Ang II alone.

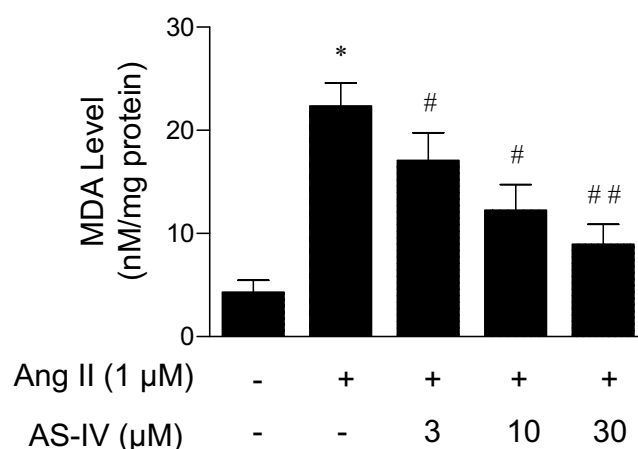


Figure 6 Effect of astragaloside IV (AS-IV) on angiotensin II (Ang II)-induced production of malondialdehyde (MDA) in endothelial cells. Human umbilical vein endothelial cells (HUVECs) were preincubated with or without AS-IV (3, 10, or 30 μ M) 1 h before incubation with Ang II (1 μ M) for 12 h. The levels of MDA in HUVECs were measured using a commercial assay kit as described in Materials and Methods. Results are expressed as means \pm SE. * p < 0.05 compared with the control group; # p < 0.05 and ## p < 0.01 compared with HUVECs exposed to Ang II alone.

occurring in inflammation is the inflammatory cells adhered to the endothelium due to the upregulation of adhesion molecules expressed on endothelial cells.^{30,31} Our findings demonstrated that AS-IV suppressed Ang II-mediated monocyte attachment to endothelial cells via attenuating the upregulation of ICAM-1 and VCAM-1. Moreover, our data showed that preincubation with AS-IV improved the dysfunction of mitochondria triggered by Ang II, thereby potentially attenuating the endothelial inflammation induced by Ang II. Overall, our novel findings show the complex interplay of AS-IV and mitochondrial function after exposure of endothelial cells to Ang II.

The vascular endothelium contributes to maintaining vascular homeostasis through the modulation of vascular tone, blood clotting, leukocyte infiltration, and permeability.^{32,33} Endothelial dysfunction is typified by diminished nitric oxide and enhanced ROS levels along with a rise in the generation/expression of proinflammatory mediators, including cytokines, chemokines, and adhesive molecules.^{4,5} Oxidative stress seems to be a crucial initiating factor for the dysfunction of endothelial cells in circulatory disorders. Usually, the dysfunction of mitochondria is considered to be the early characterization of endothelial dysfunction.^{8,34} Once deregulated, mitochondria are not only a main source but also a target of oxidative stress, thereby resulting in a vicious circle. Enhanced ROS produced from mitochondria cause injury to various intracellular constituents, which in turn accelerates ROS generation and leads to the dysfunction of mitochondria through the impairments of oxidative phosphorylation (OXPHOS) process and ATP synthesis.^{34,35} Since endothelial dysfunction and inflammation induced by enhanced mitochondrial ROS seem to contribute to circulatory pathology,^{8,34} identification of the mechanisms by which mitochondria-targeting agent AS-IV suppresses the inflammation triggered by Ang II may be helpful in developing therapeutic interventions for circulatory diseases.

The synthesis of ATP by OXPHOS process is recognized to be the main mitochondrial function. To provide energy for ATP synthesis, the transport of electrons from complexes I to IV develops MMP formed by a concentration gradient of protons across the inner mitochondrial membrane. Under pathological states, failure in electron transfer frequently results in the overproduction of mitochondrial ROS and mitochondrial dysfunction accompanied by obvious decreases in the efficiency of OXPHOS, which are derived from MMP breakdown and uncoupled OXPHOS.³⁵ In this study, our data showed that MMP and mitochondrial ATP synthesis were markedly decreased after exposure of endothelial cells to Ang II. The Ang II-triggered decreases in MMP and mitochondrial ATP synthesis were associated with the accumulation of mitochondrial ROS. According to diminished overproduction of mitochondrial ROS, AS-IV preincubation inhibited the endothelial MMP depolarization triggered by Ang II and induced an increment of ATP synthesis by enhancing the activities of OXPHOS-related enzymes, such as complexes I and III. Therefore, these studies show the protective actions of AS-IV on mitochondria after exposure of endothelial cells to Ang II.

Mitochondria are not only ATP-producing organelles, but also they contribute to regulating cell signaling via the low levels of mitochondrial ROS.^{36,37} Conversely, high concentrations of mitochondrial ROS are able to impose damage to

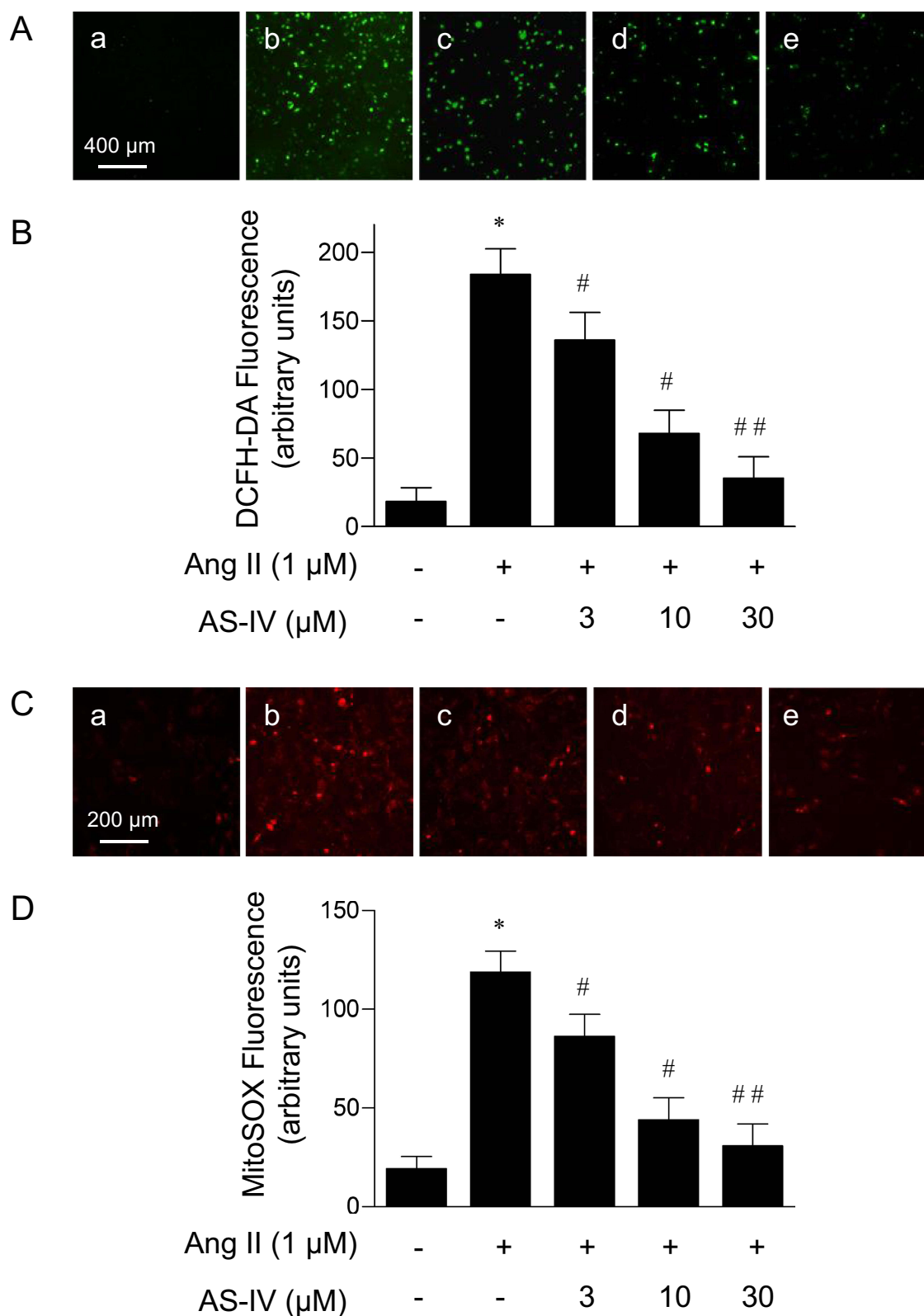


Figure 7 Effect of astragaloside IV (AS-IV) on angiotensin II (Ang II)-induced production of intracellular reactive oxygen species (**A** and **B**) and mitochondrial superoxide (**C** and **D**) in endothelial cells. Human umbilical vein endothelial cells (HUVECs) were preincubated with or without AS-IV (3, 10, or 30 μM) 1 h before incubation with Ang II (1 μM) for 12 h, and subsequently subjected to DCFH-DA or MitoSOX Red staining. (**A** and **C**) Fluorescent images of HUVECs stained with DCFH-DA or MitoSOX Red were visualized with a fluorescence microscope at 488/525 nm or 510/580 nm. Magnification, × 200. HUVECs were incubated with (a) a vehicle (control), (b) Ang II alone, Ang II with AS-IV at the concentration of (c) 3, (d) 10, or (e) 30 μM before being stained with DCFH-DA or MitoSOX Red. (**B** and **D**) Fluorescence intensity of HUVECs stained with DCFH-DA or MitoSOX Red was quantified for each image using ImageJ software. Results are expressed as means ± SE. **p* < 0.05 compared with the control group; #*p* < 0.05 and ##*p* < 0.01 compared with HUVECs exposed to Ang II alone.

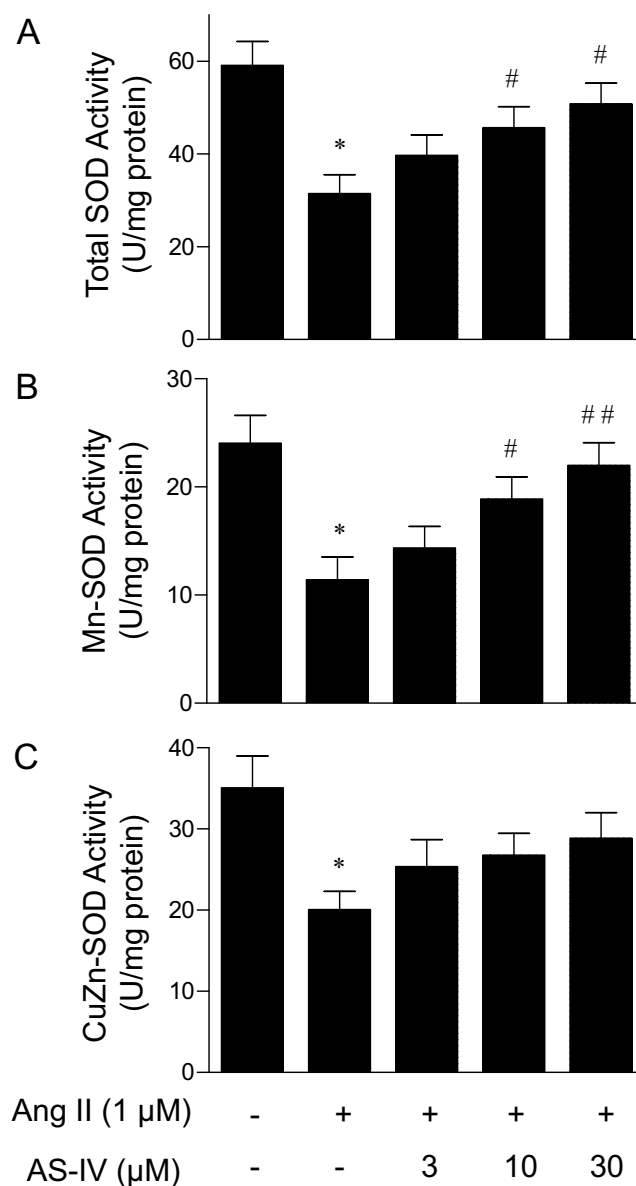


Figure 8 Effect of astragaloside IV (AS-IV) on angiotensin II (Ang II)-induced decreases in the activities of total SOD (A), Mn-SOD (B), and CuZn-SOD (C) in endothelial cells. Human umbilical vein endothelial cells (HUVECs) were preincubated with or without AS-IV (3, 10, or 30 μM) 1 h before incubation with Ang II (1 μM) for 12 h. The activities of total SOD, Mn-SOD, and CuZn-SOD in HUVECs were measured using a commercial assay kit as described in Materials and Methods. Results are expressed as means ± SE. **p* < 0.05 compared with the control group; #*p* < 0.05 and ##*p* < 0.01 compared with HUVECs exposed to Ang II alone.

mitochondria under pathological conditions. The Ang II-triggered overproduction mitochondrial ROS can impair the function of endothelial cells, thereby resulting in the onset of inflammation.¹³ It is well recognized that the sites of mitochondrial ROS generation are primarily located in the mitochondrial electron transport chain (ETC). Although most electrons arrive at the end complex IV through ETC, the electrons leaked from ETC can interact with oxygen, mainly at the site of ETC complexes I and III, to produce superoxide.^{37,38} In agreement with previous reports,^{12,39} our data demonstrated that Ang II-mediated endothelial inflammation, as evidenced by enhanced inflammatory factor production and monocyte attached to HUVECs, was associated with the diminished mitochondrial function and enhanced formation of mitochondrial ROS. The results imply that the inflammatory response induced by Ang II occurs through the mechanisms that determine a reduction of mitochondrial function and an increment of mitochondrial ROS production. About the impacts of AS-IV on Ang II-induced mitochondrial dysfunction, this study demonstrated that preincubation with AS-IV ameliorated mitochondrial function and suppressed the accumulation of mitochondrial ROS, as shown by the

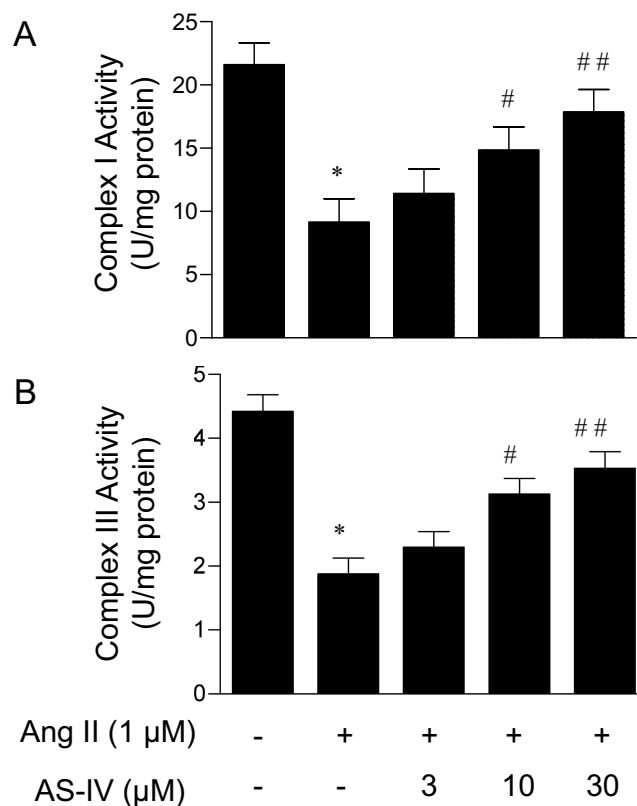


Figure 9 Effect of astragaloside IV (AS-IV) on angiotensin II (Ang II)-induced decreases in the activities of complexes I (A) and III (B) in endothelial cells. Human umbilical vein endothelial cells (HUVECs) were preincubated with or without AS-IV (3, 10, or 30 μM) 1 h before incubation with Ang II (1 μM) for 12 h. The activities of complexes I and III in HUVECs were measured using a commercial assay kit as described in Materials and Methods. Results are expressed as means ± SE. **p* < 0.05 compared with the control group; #*p* < 0.05 and ##*p* < 0.01 compared with HUVECs exposed to Ang II alone.

diminished MitoSOX fluorescence staining. Collectively, our results point out the potential action of mitochondrial dysfunction and its mediated overproduction of mitochondrial ROS in endothelial inflammation triggered by Ang II and suggest that the protective effect of AS-IV on endothelial mitochondria may mediate its antiinflammatory actions.

Under normal conditions, low levels of mitochondrial ROS, a byproduct of mitochondrial energy production, are derived from electron transport through ETC. To maintain the low levels of oxidative stress, multiple antioxidant systems existing in mitochondria work to scavenge mitochondrial ROS. Usually, mitochondrial superoxide can be converted to hydrogen peroxide by mitochondrial Mn-SOD. Hydrogen peroxide is thought to be the less reactive form of ROS.^{36,37} As before, incubation with Ang II triggered mitochondrial ROS generation in this study, however, this response was attenuated by preincubation with AS-IV. The observed decreases in superoxide and hydrogen peroxide, a product of superoxide dismutation, could be due to both decreased production and increased scavenging. We found the improvement of mitochondrial function induced by AS-IV supporting decreased superoxide production during OXPHOS. Moreover, consistent with the diminished superoxide concentrations, our findings showed that AS-IV enhanced the activity of Mn-SOD activity in HUVECs exposed to Ang II in this study. This result is consistent with previous data demonstrating the impacts of AS-IV on the activation of antioxidant enzymes.^{40,41} These data suggested that the AS-IV-induced improvement of the mitochondrial antioxidant system involving SOD could impact cellular redox balance.

NF-κB, a nuclear transcription factor sensitive to the cellular oxidative stress, is recognized to modulate the generation/expression of inflammatory mediators implicated in inflammation.^{42,43} An augmentation of ROS, including mitochondrial ROS, can activate NF-κB pathway, thereby promoting the synthesis of inflammatory factors and inducing inflammation.^{5,44,45} Our findings demonstrated that AS-IV ameliorated the mitochondrial dysfunction triggered by Ang II and suppressed its associated enhancement of mitochondrial ROS. In addition, our data also showed that AS-IV obviously suppressed the NF-κB activation induced by Ang II. Thus, the attenuating impacts of AS-IV on the endothelial

inflammation triggered by Ang II could be derived from its action in the inhibition of mitochondrial ROS production and its associated NF- κ B activation.

The complex interactions among inflammation, autophagy, and pyroptosis have been shown in various pathological processes.^{46–48} It has been demonstrated that mitochondrial dysfunction, decreased autophagy, and pyroptosis lead to in the development of inflammation.^{5,46–48} In addition to suppression of pyroptosis in various tissues,^{49,50} AS-IV was also found to inhibit lung inflammation.⁴⁶ Moreover, the inhibitory effect of AS-IV on inflammation was reversed by autophagy inhibitor. These data suggest that the antiinflammatory actions of AS-IV may be mediated by the autophagy mechanism. In this study, only in vitro experiments were performed to investigate the pharmacological mechanisms of AS-IV. Thus, further studies conducted in animal models of cardiovascular diseases such as atherosclerosis and hypertension are required to determine the detailed mechanisms for the effects of AS-IV on mitochondria, autophagy and pyroptosis in inflammation triggered by Ang II.

Overall, this study supplies comprehensive insight into the antiinflammatory activity of AS-IV and its effects on mitochondrial function. Our data revealed that AS-IV displayed obvious inhibitory effects on Ang II-mediated endothelial inflammation possibly via the improvement of mitochondrial dysfunction. These data ameliorate our current knowledge on the potential impacts of AS-IV on the endothelial inflammation triggered by Ang II. Furthermore, our data highlight the potential actions of mitochondria-targeting AS-IV in the treatment of inflammation-characterized cardiovascular diseases induced by Ang II.

Perspectives

Since enhanced mitochondrial ROS generation seems to be a critical event in Ang II-induced inflammation implicated in cardiovascular diseases, identification of the mechanisms by which AS-IV, a mitochondrial-targeting agent, inhibits the inflammation triggered by Ang II may be helpful for the development of therapeutic interventions for Ang II-associated cardiovascular diseases. In this study, our data provide new understanding of the pharmacological action of AS-IV in attenuating the development of Ang II-mediated inflammation and its possible mechanisms, leading to promoting the application of AS-IV in clinical practice.

Abbreviations

Ang II, Angiotensin II; AS-IV, Astragaloside IV; AT1R, Type-1 angiotensin receptors; CDSE, Carboxyfluorescein diacetate succinimidyl ester; DMSO, Dimethyl sulfoxide; ETC, Electron transport chain; EBM-2, Endothelial basal medium-2; FBS, Fetal bovine serum; HUVECs, Human umbilical vein endothelial cells; MDA, Malondialdehyde; MMP, Mitochondrial membrane potential; MTT, 3-(4,5-dimethylthiazol-2-yl)-2,5-Diphenyltetrazolium bromide; NF- κ B, Nuclear factor-kappa B; OXPHOS, Oxidative phosphorylation; PBS, Phosphate-buffered saline; ROS, Reactive oxygen species; SOD, Superoxide dismutase.

Acknowledgments

This study was funded by the National Nature Science Foundation of China (No. 82074194 & 81673734) to YW. This paper has been uploaded to SSRN as a preprint: https://papers.ssrn.com/sol3/papers.cfm?abstract_id=4272729.

Author Contributions

All authors made a significant contribution to the work reported, whether that is in the conception, study design, execution, acquisition of data, analysis and interpretation, or in all these areas; took part in drafting, revising or critically reviewing the article; gave final approval of the version to be published; have agreed on the journal to which the article has been submitted; and agree to be accountable for all aspects of the work.

Disclosure

The authors have no conflict of interest pertaining to this manuscript.

References

- Mendis S, Graham I, Narula J. Addressing the global burden of cardiovascular diseases; need for scalable and sustainable frameworks. *Glob Heart*. 2022;17(1):48. doi:10.5334/gh.1139
- Teo KK, Rafiq T. Cardiovascular risk factors and prevention: a perspective from developing countries. *Can J Cardiol*. 2021;37(5):733–743. doi:10.1016/j.cjca.2021.02.009
- Akhmerov A, Parimon T. Extracellular vesicles, inflammation, and cardiovascular disease. *Cells*. 2022;11(14):2229. doi:10.3390/cells11142229
- Steven S, Frenis K, Oelze M, et al. Vascular inflammation and oxidative stress: major triggers for cardiovascular disease. *Oxid Med Cell Longev*. 2019;2019:7092151. doi:10.1155/2019/7092151
- Marchio P, Guerra-Ojeda S, Vila JM, Aldasoro M, Victor VM, Mauricio MD. Targeting early atherosclerosis: a focus on oxidative stress and inflammation. *Oxid Med Cell Longev*. 2019;2019:8563845. doi:10.1155/2019/8563845
- Poredos P, Poredos AV, Gregoric I. Endothelial dysfunction and its clinical implications. *Angiology*. 2021;72(7):604–615. doi:10.1177/0003319720987752
- Joffre J, Hellman J. Oxidative stress and endothelial dysfunction in sepsis and acute inflammation. *Antioxid Redox Signal*. 2021;35(15):1291–1307. doi:10.1089/ars.2021.0027
- Salnikova D, Orekhova V, Grechko A, et al. Mitochondrial dysfunction in vascular wall cells and its role in atherosclerosis. *Int J mol Sci*. 2021;22(16):8990. doi:10.3390/ijms22168990
- Shemiakova T, Ivanova E, Grechko AV, Gerasimova EV, Sobenin IA, Orekhov AN. Mitochondrial dysfunction and DNA damage in the context of pathogenesis of atherosclerosis. *Biomedicines*. 2020;8(6):166. doi:10.3390/biomedicines8060166
- Cojocaru KA, Luchian I, Goriuc A, et al. Mitochondrial dysfunction, oxidative stress, and therapeutic strategies in diabetes, obesity, and cardiovascular disease. *Antioxidants*. 2023;12(3):658. doi:10.3390/antiox12030658
- Forrester SJ, Booz GW, Sigmund CD, et al. Angiotensin II signal transduction: an update on mechanisms of physiology and pathophysiology. *Physiol Rev*. 2018;98(3):1627–1738. doi:10.1152/physrev.00038.2017
- Cooper HA, Cicalese S, Preston KJ, et al. Targeting mitochondrial fission as a potential therapeutic for abdominal aortic aneurysm. *Cardiovasc Res*. 2021;117(3):971–982. doi:10.1093/cvr/cvaa133
- Miyao M, Cicalese S, Kawai T, et al. Involvement of senescence and mitochondrial fission in endothelial cell pro-inflammatory phenotype induced by angiotensin II. *Int J mol Sci*. 2020;21(9):3112. doi:10.3390/ijms21093112
- Zhu Z, Liang W, Chen Z, et al. Mitoquinone protects podocytes from angiotensin II-induced mitochondrial dysfunction and injury via the Keap1-Nrf2 signaling pathway. *Oxid Med Cell Longev*. 2021;2021:1394486. doi:10.1155/2021/1394486
- Dikalov SI, Nazarewicz RR. Angiotensin II-induced production of mitochondrial reactive oxygen species: potential mechanisms and relevance for cardiovascular disease. *Antioxid Redox Signal*. 2013;19(10):1085–1094. doi:10.1089/ars.2012.4604
- Yang Y, Hong M, Lian WW, Chen Z. Review of the pharmacological effects of astragaloside IV and its autophagic mechanism in association with inflammation. *World J Clin Cases*. 2022;10(28):10004–10016. doi:10.12998/wjcc.v10.i28.10004
- Zhang J, Wu C, Gao L, Du G, Qin X. Astragaloside IV derived from *Astragalus membranaceus*: a research review on the pharmacological effects. *Adv Pharmacol*. 2020;87:89–112.
- Li L, Hou X, Xu R, Liu C, Tu M. Research review on the pharmacological effects of astragaloside IV. *Fundam Clin Pharmacol*. 2017;31(1):17–36. doi:10.1111/fcp.12232
- Wang J, Zhou Y, Wu S, et al. Astragaloside IV attenuated 3,4-benzopyrene-induced abdominal aortic aneurysm by ameliorating macrophage-mediated inflammation. *Front Pharmacol*. 2018;9:496. doi:10.3389/fphar.2018.00496
- Zhang Y, Tao C, Xuan C, Jiang J, Cao W. Transcriptomic analysis reveals the protection of astragaloside IV against diabetic nephropathy by modulating inflammation. *Oxid Med Cell Longev*. 2020;2020:9542165. doi:10.1155/2020/9542165
- Wang E, Wang L, Ding R, et al. Astragaloside IV acts through multi-scale mechanisms to effectively reduce diabetic nephropathy. *Pharmacol Res*. 2020;157:104831. doi:10.1016/j.phrs.2020.104831
- Murata I, Abe Y, Yaginuma Y, et al. Astragaloside-IV prevents acute kidney injury and inflammation by normalizing muscular mitochondrial function associated with a nitric oxide protective mechanism in crush syndrome rats. *Ann Intensive Care*. 2017;7(1):90. doi:10.1186/s13613-017-0313-2
- Feng M, Lv J, Zhang C, et al. Astragaloside IV protects sepsis-induced acute kidney injury by attenuating mitochondrial dysfunction and apoptosis in renal tubular epithelial cells. *Curr Pharm Des*. 2022;28(34):2825–2834. doi:10.2174/1381612828666220902123755
- Mosmann T. Rapid colorimetric assay for cellular growth and survival: application to proliferation and cytotoxicity assays. *J Immunol Methods*. 1983;65(1–2):55–63. doi:10.1016/0022-1759(83)90303-4
- Wang Y, Cui L, Xu H, et al. TRPV1 agonism inhibits endothelial cell inflammation via activation of eNOS/NO pathway. *Atherosclerosis*. 2017;260:13–19. doi:10.1016/j.atherosclerosis.2017.03.016
- Zhang S, Xie S, Gao Y, Wang Y. Triptolide alleviates oxidized LDL-induced endothelial inflammation by attenuating the oxidative stress-mediated nuclear factor-Kappa B pathway. *Curr Ther Res Clin Exp*. 2022;97:100683. doi:10.1016/j.curtheres.2022.100683
- Kumar A, Noda K, Philips B, et al. Nitrite attenuates mitochondrial impairment and vascular permeability induced by ischemia-reperfusion injury in the lung. *Am J Physiol Lung Cell mol Physiol*. 2020;318(4):L580–L591. doi:10.1152/ajplung.00367.2018
- Kim S, Iwao H. Molecular and cellular mechanisms of angiotensin II-mediated cardiovascular and renal diseases. *Pharmacol Rev*. 2000;52(1):11–34. doi:10.1016/S0031-6997(24)01434-0
- Robles-Vera I, Toral M, de la Visitación N, Aguilera-Sánchez N, Redondo JM, Duarte J. Protective effects of short-chain fatty acids on endothelial dysfunction induced by angiotensin II. *Front Physiol*. 2020;11:277. doi:10.3389/fphys.2020.00277
- Wang L, Cheng CK, Yi M, Liu KO, Huang Y. Targeting endothelial dysfunction and inflammation. *J mol Cell Cardiol*. 2022;168:58–67. doi:10.1016/j.yjmcc.2022.04.011
- Gerhardt T, Ley K. Monocyte trafficking across the vessel wall. *Cardiovasc Res*. 2015;107(3):321–330. doi:10.1093/cvr/cvv147
- Theofilis P, Sagris M, Oikonomou E, et al. Inflammatory mechanisms contributing to endothelial dysfunction. *Biomedicines*. 2021;9(7):781. doi:10.3390/biomedicines9070781

33. Marziano C, Genet G, Hirschi KK. Vascular endothelial cell specification in health and disease. *Angiogenesis*. 2021;24(2):213–236. doi:10.1007/s10456-021-09785-7
34. Kirkman DL, Robinson AT, Rossman MJ, Seals DR, Edwards DG. Mitochondrial contributions to vascular endothelial dysfunction, arterial stiffness, and cardiovascular diseases. *Am J Physiol Heart Circ Physiol*. 2021;320(5):H2080–100. doi:10.1152/ajpheart.00917.2020
35. Szewczyk A, Jarmuszkiewicz W, Koziel A, et al. Mitochondrial mechanisms of endothelial dysfunction. *Pharmacol Rep*. 2015;67(4):704–710. doi:10.1016/j.pharep.2015.04.009
36. Harrington JS, Ryter SW, Platakis M, Price DR, Choi AMK. Mitochondria in health, disease, and aging. *Physiol Rev*. 2023;103(4):2349–2422. doi:10.1152/physrev.00058.2021
37. Chenna S, Koopman WJH, Prehn JHM, Connolly NMC. Mechanisms and mathematical modeling of ROS production by the mitochondrial electron transport chain. *Am J Physiol Cell Physiol*. 2022;323(1):C69–83. doi:10.1152/ajpcell.00455.2021
38. Brand MD. Mitochondrial generation of superoxide and hydrogen peroxide as the source of mitochondrial redox signaling. *Free Radic Biol Med*. 2016;100:14–31. doi:10.1016/j.freeradbiomed.2016.04.001
39. Beak JY, Kang HS, Huang W, et al. The nuclear receptor ROR α protects against angiotensin II-induced cardiac hypertrophy and heart failure. *Am J Physiol Heart Circ Physiol*. 2019;316(1):H186–200. doi:10.1152/ajpheart.00531.2018
40. Xu N, Kan P, Yao X, et al. Astragaloside IV reversed the autophagy and oxidative stress induced by the intestinal microbiota of AIS in mice. *J Microbiol*. 2018;56(11):838–846. doi:10.1007/s12275-018-8327-5
41. Li L, Huang T, Yang J, et al. PINK1/Parkin pathway-mediated mitophagy by AS-IV to explore the molecular mechanism of muscle cell damage. *Biomed Pharmacother*. 2023;161:114533. doi:10.1016/j.biopha.2023.114533
42. Zhang Q, Lenardo MJ, Baltimore D. 30 years of NF- κ B: a blossoming of relevance to human pathobiology. *Cell*. 2017;168(1–2):37–57. doi:10.1016/j.cell.2016.12.012
43. Bacher S, Meier-Selch J, Kracht M, Schmitz ML. Regulation of transcription factor NF- κ B in its natural habitat: the nucleus. *Cells*. 2021;10(4):753. doi:10.3390/cells10040753
44. Kastl L, Sauer SW, Ruppert T, et al. TNF- α mediates mitochondrial uncoupling and enhances ROS-dependent cell migration via NF- κ B activation in liver cells. *FEBS Lett*. 2014;588(1):175–183. doi:10.1016/j.febslet.2013.11.033
45. Zeng Y, Zhu G, Zhu M, et al. Edaravone attenuated particulate matter-induced lung inflammation by inhibiting ROS-NF- κ B signaling pathway. *Oxid Med Cell Longev*. 2022;2022:6908884. doi:10.1155/2022/6908884
46. Wang Z, Wu Y, Pei C, et al. Astragaloside IV pre-treatment attenuates PM_{2.5}-induced lung injury in rats: impact on autophagy, apoptosis and inflammation. *Phytomedicine*. 2022;96:153912. doi:10.1016/j.phymed.2021.153912
47. Shen Y, Malik SA, Amir M, et al. Decreased hepatocyte autophagy leads to synergistic IL-1 β and TNF mouse liver injury and inflammation. *Hepatology*. 2020;72(2):595–608. doi:10.1002/hep.31209
48. Wei Y, Lan B, Zheng T, et al. GSDME-mediated pyroptosis promotes the progression and associated inflammation of atherosclerosis. *Nat Commun*. 2023;14(1):929. doi:10.1038/s41467-023-36614-w
49. Zhang X, Qu H, Yang T, Liu Q, Zhou H. Astragaloside IV attenuate MI-induced myocardial fibrosis and cardiac remodeling by inhibiting ROS/caspase-1/GSDMD signaling pathway. *Cell Cycle*. 2022;21(21):2309–2322. doi:10.1080/15384101.2022.2093598
50. Xiao L, Dai Z, Tang W, Liu C, Tang B. Astragaloside IV alleviates cerebral ischemia-reperfusion injury through NLRP3 inflammasome-mediated pyroptosis inhibition via activating Nrf2. *Oxid Med Cell Longev*. 2021;2021:9925561. doi:10.1155/2021/9925561